












Cite this: *Dalton Trans.*, 2019, **48**,
4611

Lanthanide complexes with phenanthroline-based ligands: insights into cell death mechanisms obtained by microscopy techniques†

Maria Paula Cabral Campello, *‡^a Elisa Palma, ^{a,b} Isabel Correia, ^b Pedro M. R. Paulo, ^b António Matos, ^c José Rino, ^d Joana Coimbra, ^e João Costa Pessoa, ^b Dinorah Gambino, ^f António Paulo ^a and Fernanda Marques *‡^a

Herein we report the synthesis, characterization, and photophysical and biological evaluation of the complexes $\text{Ln}(\text{DBM})_3(\text{RPhen})$ ($\text{Ln} = \text{Sm}$, $\text{R} = \text{H}$; $\text{Ln} = \text{Sm}$, Eu , Tb , $\text{R} = 5\text{-NH}_2$) stabilized by three β -diketonate units (DBM) and a phenanthroline (RPhen) derivative, with the aim of contributing to the development of lanthanide-based compounds with potential application as anticancer agents. The UV-vis spectra of $[\text{Sm}(\text{DBM})_3(\text{Phen})]$, $[\text{Sm}(\text{DBM})_3(\text{NH}_2\text{Phen})]$, $[\text{Eu}(\text{DBM})_3(\text{NH}_2\text{Phen})]$ and $[\text{Tb}(\text{DBM})_3(\text{NH}_2\text{Phen})]$ measured in DMSO and PBS showed a strong absorption band centered at ca. 350 nm in both solvents. In DMSO, all lanthanide compounds except $[\text{Sm}(\text{DBM})_3(\text{Phen})]$ show a ligand centered emission band at ca. 520 nm. In PBS only sharp emission peaks are detected. The complexes show similar cytotoxic effects in A2780 ovarian cancer cells, presenting IC_{50} values at 24 h in the range 16–27 μM . The measurement of the cellular uptake of the complexes in the A2780 cells by inductively coupled plasma mass spectrometry (ICP-MS) revealed preferential accumulation at the membrane and cytoskeleton, with the exception of $[\text{Sm}(\text{DBM})_3(\text{Phen})]$ that presented higher accumulation in the cytosol than in the cell membranes. All the evaluated lanthanide complexes showed low nuclear uptake, although not negligible. Spectroscopic studies on the interaction of the complexes with calf thymus DNA (ctDNA) revealed a moderate affinity with apparent binding constants in the 10^4 M^{-1} range. Complexes bind DNA not by intercalation but probably by electrostatic interactions. A morphological evaluation of the cells treated with the different complexes by electron microscopy (TEM/SEM) proved that all of them induce mitochondrial alterations, which seemed more pronounced for the NH_2Phen complexes. In addition, the complex $[\text{Eu}(\text{DBM})_3(\text{NH}_2\text{Phen})]$ presented lysosomal uptake that might explain its augmented cytotoxicity.

Received 12th February 2019,

Accepted 7th March 2019

DOI: 10.1039/c9dt00640k

rsc.li/dalton

Introduction

Medicinal chemistry is one of the most challenging areas of research that focus on the design and evaluation of organic and inorganic compounds aimed at the development of new drugs for diagnosis and therapy. In this field, the evaluation of the interactions of drugs with biological systems and the relationship between their chemical structure and biological effects [structure–activity relationship (SAR)] is of paramount importance and has received increasing attention in the last few years.¹

Cisplatin represents the landmark of metal-based chemotherapeutics and is still the most widely prescribed anti-cancer drug.² Severe side effects and drug resistance reported for cisplatin have prompted numerous researchers to develop cisplatin analogues in order to collapse the net balance observed for the therapeutic efficacy of cisplatin vs. side effects

^aCentro de Ciências e Tecnologias Nucleares, Instituto Superior Técnico, Universidade de Lisboa, Estrada Nacional 10, km 139.7, 2695-066 Bobadela LRS, Portugal. E-mail: fmarujo@ctn.tecnico.ulisboa.pt, pcampelo@ctn.tecnico.ulisboa.pt

^bCentro de Química Estrutural, Instituto Superior Técnico, Universidade de Lisboa, Av. Rovisco Pais, 1049-001 Lisboa, Portugal

^cCentro de Investigação Interdisciplinar Egas Moniz, Campus Universitário, Quinta da Granja, Monte de Caparica, Almada, Portugal

^dFaculdade de Medicina da Universidade de Lisboa, Instituto de Medicina Molecular Faculdade de Medicina de Lisboa Av. Prof. Egas Moniz, 1649-028 Lisboa, Portugal

^eLaboratório Central de Análises, Universidade de Aveiro, 3810-193 Aveiro, Portugal

^fCátedra de Química Inorgánica, Facultad de Química, Universidad de la República, 11800 Montevideo, Uruguay

†Electronic supplementary information (ESI) available. See DOI: 10.1039/c9dt00640k

‡These authors contributed equally to this work.

and drug resistance.^{3,4} The use of transition metals other than platinum (*e.g.*, V, Ru, Cu, and Au) has also triggered intensive research in the modern era of metal-based anticancer compounds.^{5–11} Ruthenium compounds have received great attention as antitumor agents with high potential against solid tumors or selective antimetastatic properties, particularly [ImH][*trans*-RuCl₄(DMSO)Im] (NAMI-A) and [ImH][*trans*-RuCl₄(Im)₂] (KP1019) (where Im = imidazole) that have progressed to clinical evaluation.^{12–14} Based on studies with these and other related compounds it has been shown that the biological activity of metal-based drugs, including cisplatin, is not only centered on their interaction with DNA but also on many other biomolecular targets and factors like pH and the redox environment of tumor cells that could be even more relevant than their DNA interaction.^{15–20}

Along with transition metals, lanthanides can offer remarkable opportunities since it is well recognized that these 4f elements have interesting physico-chemical properties and accordingly diverse lanthanide compounds have been evaluated for a myriad of applications both in the technological field (sensor devices, optical fibers, lasers, *etc.*) and in the medical field, specifically in diagnosis and therapy.^{21–37} Lanthanide complexes bearing N-heterocyclic ligands as chromophores were also evaluated as DNA nucleases, cytotoxic drugs or photosensitizers in photodynamic therapy (PDT), but there are still only a few reports addressing these topics. The potential of lanthanide complexes for this type of applications is strongly dependent on the metal center, chromophore, and on the stabilizing ligands.^{36–40}

Luminescence is one of the remarkable characteristics of trivalent lanthanide ions; apart from La³⁺ and Lu³⁺, all the other trivalent lanthanide ions show ubiquitous luminescence. Electronically excited Gd³⁺ emits in the UV region, Pr³⁺, Sm³⁺, Eu³⁺, Tb³⁺, Dy³⁺ and Tm³⁺ emit in the visible region and Nd³⁺, Ho³⁺, Er³⁺ and Yb³⁺ in the NIR region.²⁴ However, it can be quite challenging to achieve an efficient photoexcitation of the lanthanide ions due to the forbidden f-f transitions, by Laporte's rule; this results in low extinction coefficients. Considerable enhancement of luminescence emission has been largely achieved by the improvement of the *antenna effect*, namely by the incorporation of lanthanide ions into polydentate ligands bearing organic chromophores to promote the transfer of the absorbed energy into the lanthanide ions.²⁵ Among the lanthanide series, the complexes of Eu³⁺ and Tb³⁺ ions exhibit stability and photophysical properties and are of special interest as luminescent probes in clinical diagnostics and accordingly they have probably been the most evaluated.^{40–44}

For instance, the lanthanide luminescence can be based on N-heterocyclic chromophores such as pyridine, bipyridine, terpyridine, phenanthroline and benzimidazole, most of them associated with β-diketonate ligands. In general, the luminescence of the lanthanide complexes stabilized with aromatic β-diketones is more intense than that shown by the complexes stabilized with the congener aliphatic β-diketonate ligands.^{45–49} For more than a century, this latter class of com-

plexes has been explored mostly by physicists interested in assessing their potential capabilities as electronic devices. However, the experimental synthetic procedure to obtain such compounds is often absent in a large number of publications or, when reported, leads mainly to impure products or compounds with poorly defined composition.^{46–49}

Within our research activities in the medicinal inorganic chemistry field, we have evaluated the antimicrobial and antitumoral potential of several transition metal complexes bearing N-heterocyclic ligands.^{50–55} Studies of polypyridyl complexes of the type [M(SalGly)(RPhen)] (M = Cu, Zn, V) (SalGly = *N*-salicylidene-glycinate) (RPhen = phenanthroline and phenanthroline derivatives) by analytical and imaging techniques revealed that the cellular uptake and the mechanisms of cell death were dependent on the metal center.⁵² Most of the complexes were preferentially retained at the membranes. Notwithstanding, [Cu(SalGly)(Phen)] showed a high cellular uptake combined with a significant accumulation in the nucleus that probably explain the remarkable cytotoxic activity of this complex.⁵² Altogether, all these findings prompted us to extend our studies to a family of phenanthroline-based 4f-element complexes with the aim of shedding more light on the mechanisms behind the cellular uptake and the cell death induced by this class of complexes.

Herein we report the synthesis and characterization of Sm, Eu and Tb complexes stabilized by three aromatic β-diketonate units and a phenanthroline chromophore (Fig. 1). The synthesis of this type of compound was first reported in 1964 by Melby *et al.*^{56a} However, their characterization is often absent and/or unsatisfactory. Specifically, the samarium complex tris(dibenzoylmethane) mono(1,10-phenanthroline) ([Sm(DBM)₃(Phen)] (1) was completely characterized for the first time by Stanley *et al.* in 2010, although its NMR spectra have not been reported.^{56b} Concerning related complexes bearing 1,10-phenanthroline-5-amine, to the best of our knowledge, their structural characterization has not yet been reported even for the commercially available tris(dibenzoylmethane) mono(5-amino-1,10-phenanthroline) europium(III) complex ([Eu(DBM)₃(NH₂Phen)] (3). In this contribution, we also report the *in vitro* and biological evaluation of these lanthanide complexes as potential anticancer drugs. This comprised

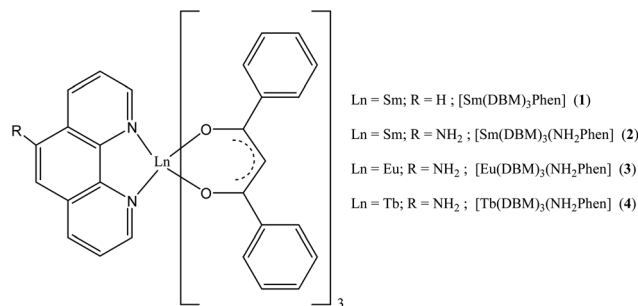


Fig. 1 Molecular structure of the lanthanide complexes [Ln(DBM)₃(RPhen)] evaluated in this study (Ln = Sm, R = H; Ln = Sm, Eu, Tb, R = 5-NH₂).

the evaluation of their DNA interactions, the measurement of their uptake and cytotoxicity in the A2780 ovarian and MDAMB231 breast cancer cells, and the assessment of their intracellular localization by confocal fluorescence microscopy and ICP-MS, as well as the study of induced mechanisms of cell death using microscopy tools.

Results and discussion

Synthesis and characterization

Aiming at exploring the anticancer potential of lanthanide complexes with β -diketonates and phenanthroline (RPhen) derivatives, we synthesized and fully characterized the four lanthanide complexes $\text{Ln}(\text{DBM})_3(\text{RPhen})$ (DBM = 1,3-diphenyl-1,3-propanedionate, Ln = Sm, R = H (**1**); Ln = Sm (**2**), Eu (**3**), Tb (**4**), R = 5-NH₂), whose structural formula is depicted in Fig. 1.

The complex tris(dibenzoylmethane) mono(1,10-phenanthroline) samarium(III) [$\text{Sm}(\text{DBM})_3(\text{Phen})$] (**1**) and the congener complexes [$\text{Sm}(\text{DBM})_3(\text{NH}_2\text{Phen})$] (**2**) and [$\text{Eu}(\text{DBM})_3(\text{NH}_2\text{Phen})$] (**3**) (NH₂Phen = 5-amino-1,10-phenanthroline) have been synthesized by one pot *in situ* reactions using slightly adapted previously reported procedures.^{56–58} All attempts to synthesize the terbium complex [$\text{Tb}(\text{DBM})_3(\text{NH}_2\text{Phen})$] (**4**) using a similar procedure failed. In the majority of the reactions performed, a pale yellow solid was obtained but neither the ESI-MS analysis nor the elemental C, H, and N analysis were consistent with the anticipated product. The terbium complex could be obtained, in moderate

yield (40%), by a two-step reaction. It was found that the method to achieve the terbium complex is the isolation of the intermediate aqua complex, $\text{Tb}(\text{DBM})_3 \cdot (\text{H}_2\text{O})_x$, formed in the first reaction step prior to the reaction with the Lewis base NH₂Phen.^{56b,59,60}

The IR spectrum of [$\text{Sm}(\text{DBM})_3(\text{Phen})$] (Fig. S1†) is in perfect concordance with that reported by Stanley *et al.*^{56b} The pattern of the IR spectra of the other three Ln compounds, [$\text{Sm}(\text{DBM})_3(\text{NH}_2\text{Phen})$] (**2**), [$\text{Eu}(\text{DBM})_3(\text{NH}_2\text{Phen})$] (**3**), and [$\text{Tb}(\text{DBM})_3(\text{NH}_2\text{Phen})$] (**4**), is very similar (see Fig. S6 and Table S1†). The assignment of the bands was made based on the data reported for HDBM, phenanthroline derivative ligands and related lanthanide complexes.^{46,47,56,61–63} The three strong broad bands in the region 1700–1300 cm⁻¹, related to the C–C stretching of the phenyl group, C=O and C=C stretching modes of HDBM, are considerably red-shifted in the three lanthanide complexes as compared with the free ligand. Concerning the bands due to the coordination of the NH₂Phen to the metal center it was observed that the band assigned to the C–N stretching vibration, appearing as a doublet at 1428 cm⁻¹ and 1407 cm⁻¹ in the free NH₂Phen, is shifted and appears as a singlet in the lanthanide complexes. The differences observed in the position and shape of the absorption bands of the lanthanide complexes relatively to the ligands are also consistent with the formation of the complexes.

The ESI-MS spectra of all the $\text{Ln}(\text{DBM})_3(\text{RPhen})$ complexes showed the presence of peaks at m/z values corresponding to the expected molecular ions (Fig. S2, S5, S9 and S11†), while

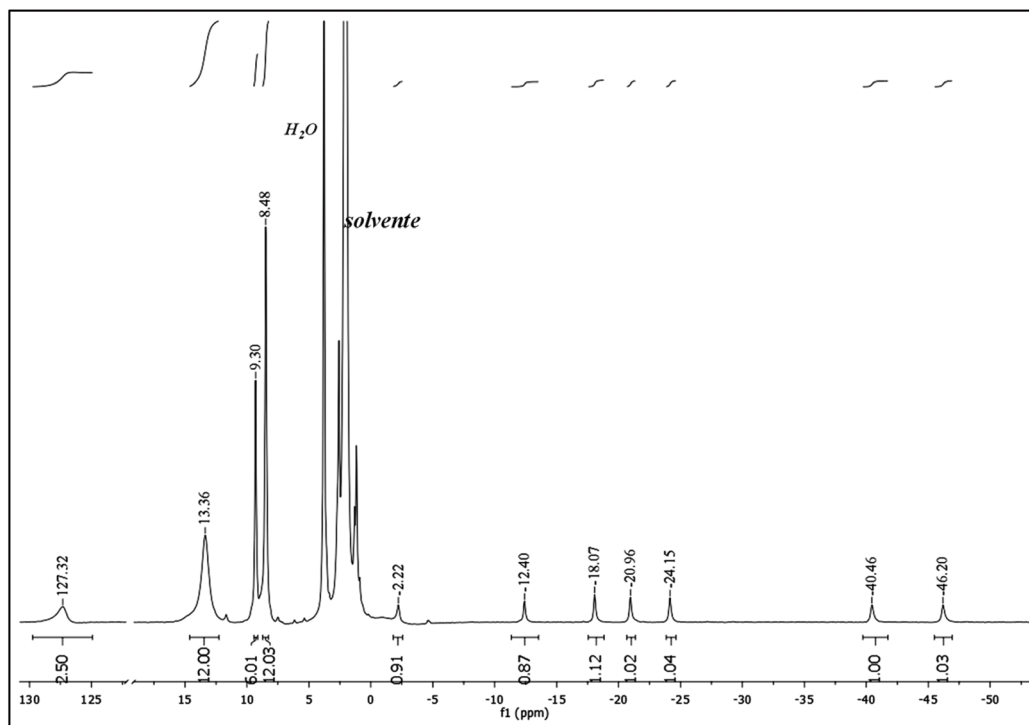


Fig. 2 ¹H NMR spectrum of [$\text{Tb}(\text{DBM})_3(\text{NH}_2\text{Phen})$] in acetone-*d*₆.

presenting splitting patterns consistent with the respective isotopic distributions. Moreover, very good agreement was found between the theoretical and experimental data for their C, H, and N elemental analyses, which corroborates the formation of the desired compounds.

The ^1H NMR spectra of all complexes are consistent with the formation of heteroleptic complexes containing one RPhen ligand and three HDBM ligands. The OH resonance observed downfield of the ^1H NMR spectrum of the enol form of HDBM is absent in all the ^1H NMR spectra of the four lanthanide complexes, as expected after coordination of the β -diketonate ligand to the metal center. The resonances of the CH methine protons are not considerably shifted in the spectra of the samarium complexes **1** and **2**; in the spectrum of the europium complex a significant shift towards the high field side is noted.

Due to the paramagnetic nature of the Tb^{3+} ion ($\mu_{\text{Tb}} = 9.72$) the proton chemical shifts in the ^1H NMR spectrum of $[\text{Tb}(\text{DBM})_3(\text{NH}_2\text{Phen})]$, recorded in acetone d_6 , spread through a range of about 160 ppm (from -46 to 127 ppm). The seven resonances due to the protons of NH_2Phen are dramatically shifted to higher field whereas the resonance due to the methine protons is shifted in the reverse direction (Fig. 2).

UV/Vis and luminescence spectroscopic studies

The UV-vis spectra of the complexes and ligands were measured in DMSO and PBS (0.01 M, pH 7.4) and are included in Fig. 3. All complexes show a strong absorption band centered at *ca.* 350 nm in both solvents. The lanthanide ions do not contribute to the absorption spectra due to the fact that f-f transitions are Laporte-forbidden and very weak (extinction coefficients $\epsilon < 1 \text{ M}^{-1} \text{ cm}^{-1}$).⁶⁴ The 350 nm band is assigned to the DBM^- ligand since this compound shows a strong absorption band in the same region.⁶⁵ NH_2Phen also absorbs in this region and contributes to the lanthanide absorption spectra.

The excitation spectra measured in DMSO for all NH_2Phen compounds are depicted in Fig. 4. All spectra are similar except for small intensity differences, exhibiting two broad bands with maxima around 280 nm and 344 nm, assigned to transitions from the NH_2Phen ligand-centered excited states.⁶⁶

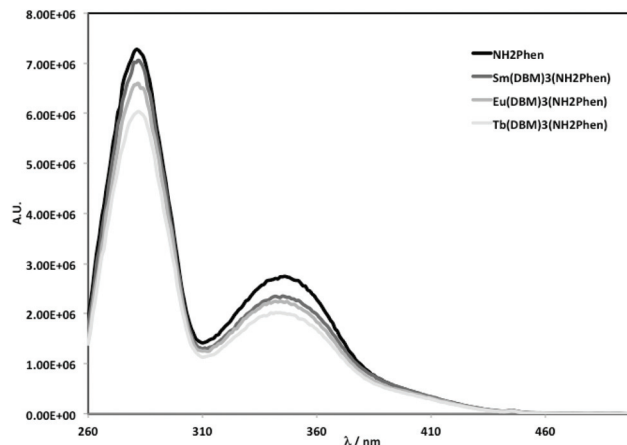


Fig. 4 Excitation spectra measured in DMSO for solutions containing the NH_2Phen compounds at concentrations of *ca.* 3×10^{-6} M. $\lambda_{\text{em}} = 515$ nm.

Free lanthanide ions yield very inefficient light absorption, except in the presence of suitable organic ligands, such as those reported here.⁶⁷ These types of ligands act as antenna, efficiently absorbing light in the UV region and transferring energy to the lanthanide ion that becomes electronically excited.⁶⁸ The luminescence emission spectra of all complexes and ligands measured in DMSO are depicted in Fig. 5a. DBM showed no luminescence, while NH_2Phen shows an intense emission band centered at 507 nm. All complexes except $[\text{Sm}(\text{DBM})_3(\text{Phen})]$ show a ligand centered emission band in the visible region at *ca.* 510 nm, which corresponds to the ligand emission. The phen ligand does not show emission in the 500 nm region.

$[\text{Sm}(\text{DBM})_3(\text{Phen})]$ shows sharp emission bands at 562, 598 and 645 nm, assigned to $^4\text{G}_{5/2} \rightarrow ^6\text{H}_{5/2}$, $^4\text{G}_{5/2} \rightarrow ^6\text{H}_{7/2}$ and $^4\text{G}_{5/2} \rightarrow ^6\text{H}_{9/2}$, with the most intense being $^4\text{G}_{5/2} \rightarrow ^6\text{H}_{9/2}$. For $[\text{Sm}(\text{DBM})_3(\text{NH}_2\text{Phen})]$ the sharp bands are overlapped with the ligand centered bands and only the $^4\text{G}_{5/2} \rightarrow ^6\text{H}_{9/2}$ band at 643 nm is clearly visible (Fig. 5b). The $[\text{Eu}(\text{DBM})_3(\text{NH}_2\text{Phen})]$ complex shows bands at 578, 599, 613 and 687 nm, assigned to $^5\text{D}_0 \rightarrow ^7\text{F}_0$, $^5\text{D}_0 \rightarrow ^7\text{F}_1$, $^5\text{D}_0 \rightarrow ^7\text{F}_2$ and $^5\text{D}_0 \rightarrow ^7\text{F}_3$, with the

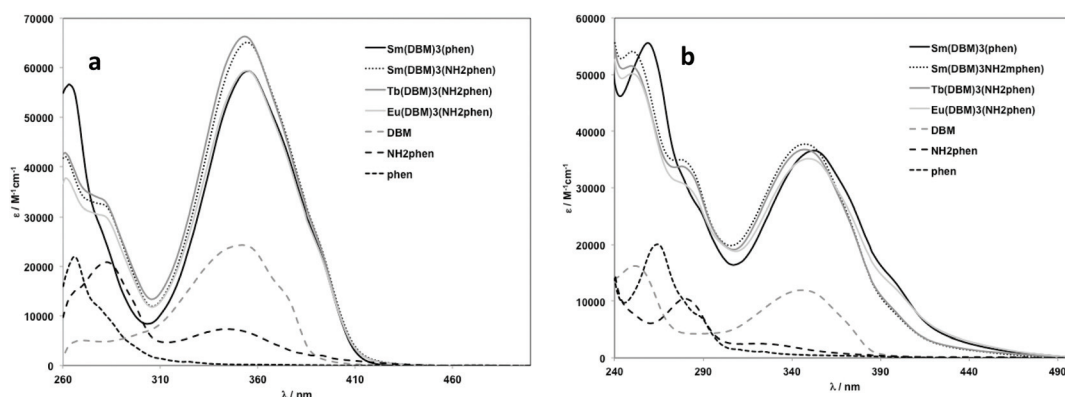


Fig. 3 UV-vis absorption spectra measured in DMSO (a) and PBS (b) for solutions of the complexes at concentrations of 1.0×10^{-5} M.

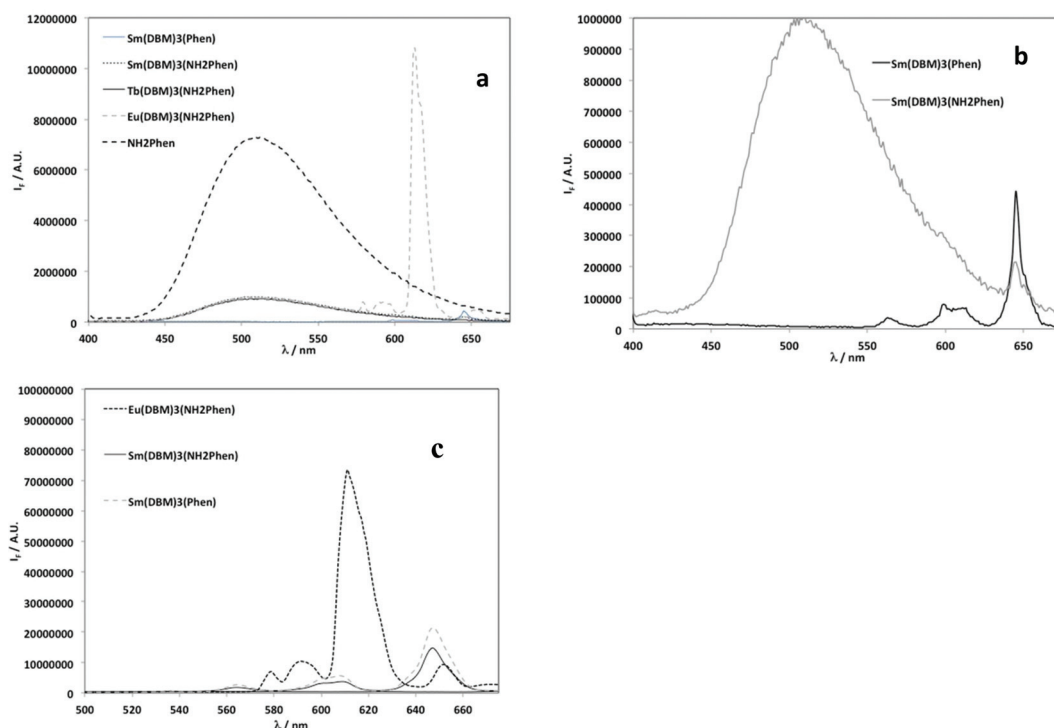


Fig. 5 Luminescence emission spectra measured in DMSO (a and b) and PBS (c) for solutions of the complexes at ca. 1.0×10^{-5} M. $\lambda_{\text{exc}} = 355$ nm and slits = 3 nm (5 nm in (c)).

most intense being the $^5D_0 \rightarrow ^7F_2$ transition. These spectroscopic features are in agreement with the ones previously reported for $[\text{Ln}(\text{NO}_2\text{Phen})_3\text{Cl}_3] \cdot 2\text{H}_2\text{O}$ complexes for which the luminescence of the europium complex was also stronger than that of the samarium complex.⁶⁶

In PBS, the ligand centered emission band is not observed and only the sharp emission peaks are present, indicating

either that the NH_2phen emission is suppressed in PBS or that efficient energy transfer from the excited state of the organic ligand to emitting states of the $\text{Ln}(\text{III})$ ions occurs. For $\text{Sm}(\text{III})$, the emission bands for both complexes are overlapped and are due to the f-f transitions $^4G_{5/2} \rightarrow ^6H_{5/2}$, $^4G_{5/2} \rightarrow ^6H_{7/2}$ and $^4G_{5/2} \rightarrow ^6H_{9/2}$ at 562, 600 and 647 nm, respectively.⁶⁹ In $\text{Eu}(\text{III})$ the emission bands originate from electronic transitions from

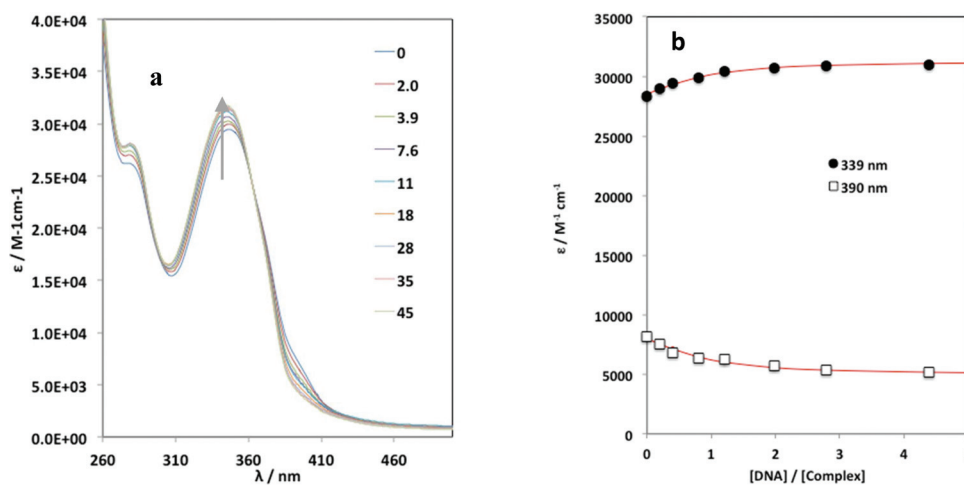


Fig. 6 (a) UV-vis spectra measured for the titration of a solution in PBS of $[\text{Sm}(\text{DBM})_3(\text{NH}_2\text{Phen})]$ (1.0×10^{-5} M) with increasing amounts of ctDNA (concentrations indicated in the legend are in μM ; the arrow indicates changes upon DNA addition), after dilution correction. The same amount of DNA was added in the reference cuvette; (b) variation of the molar absorptivity at two wavelengths (339 and 390 nm) with the $[\text{DNA}]/[\text{Complex}]$ ratio; the curves in red show the fitted model to determine the binding constants of the Ln complexes with DNA.

the lowest excited state, 5D_0 , to the multiple ground state, 7F_J ($J = 6-0$). The expected peaks are well resolved, and appear at 574, 588, 610 and 649 nm, with the band assigned to $^5D_0 \rightarrow ^7F_2$ (610 nm) being the most intense. The strong intensity observed for the hypersensitive transition, $^5D_0 \rightarrow ^7F_2$, is typical of Eu(III)-diketonate complexes.⁷⁰ For Tb(III) no luminescence was detected in this solvent.

Interaction with DNA

The lanthanide complexes contain Phen ligands, which are known to intercalate in between DNA base pairs. The complex ability to interact with DNA was evaluated by UV-vis absorption and fluorescence spectroscopy. Since in PBS the energy transfer from the ligand to the lanthanide ion is efficient and no ligand centered bands were observed, a competition assay was employed with a known intercalator, thiazole orange (TO).⁷¹ The fluorescence emission spectra were measured for systems containing ctDNA, TO and increasing amounts of complexes and for solutions containing TO and increasing amounts of complexes. However, emission spectra showed the emergence of a new band at *ca.* 580 nm that was also found to be present in the spectra of solutions containing only TO and increasing amounts of the complexes, *i.e.* without DNA (see the ESI†). This band suggests that TO interacts directly with the Ln complex, which could interfere with the competition assay that assumes that these species bind to DNA independently.

In view of this limitation, another approach was used to probe the binding of the complexes to DNA by monitoring the changes in the UV-vis absorption spectrum of solutions containing the complexes that were titrated with increasing amounts of ctDNA (see Fig. S14†). The spectra measured for $[\text{Sm}(\text{DBM})_3(\text{NH}_2\text{Phen})]$ are shown in Fig. 6a. It is clear that an isobestic point appears at *ca.* 365 nm, which indicates an equilibrium between two spectroscopic forms of Ln complexes, free and associated with DNA. The variation of the molar absorptivity is plotted in Fig. 6b at two selected wavelengths.

Table 1 IC_{50} values (μM) obtained for the Ln complexes after 24 h and 48 h incubation times using the MTT assay. Results are the mean \pm SD of two independent experiments performed with at least six replicates per concentration

Compounds	IC_{50} (μM)			
	A2780		MDAMB231	
	24 h	48 h	24 h	48 h
$\text{Sm}(\text{DBM})_3(\text{Phen})$	17.7 ± 3.1	5.3 ± 1.1	63.5 ± 5.5	11.1 ± 4.2
$\text{Sm}(\text{DBM})_3(\text{NH}_2\text{Phen})$	22.5 ± 4.5	6.3 ± 1.2	79.6 ± 6.5	6.9 ± 2.2
$\text{Eu}(\text{DBM})_3(\text{NH}_2\text{Phen})$	16.4 ± 2.6	0.6 ± 0.1	>100	0.9 ± 0.4
$\text{Tb}(\text{DBM})_3(\text{NH}_2\text{Phen})$	26.9 ± 5.5	1.0 ± 0.2	>100	4.0 ± 2.5
Phen	>100	7.6 ± 1.5	>100	22.5 ± 8.0
NH_2Phen	60.7 ± 10	9.5 ± 1.5	>100	17.0 ± 5.5
SmCl_3	>100	>100	>100	>100
TbCl_3	>100	>100	>100	>100
EuCl_3	>100	>100	>100	>100
Cisplatin	26.7 ± 8.0	20.7 ± 5.6	104 ± 16	13.8 ± 4.5

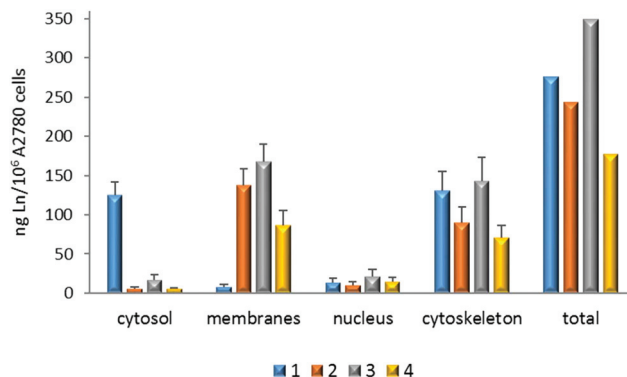


Fig. 7 Cellular uptake of the lanthanide complexes (ng per million A2780 cells). Results are the mean \pm SD of two independent experiments.

These results were used to determine binding constants for the association of Ln complexes with DNA assuming the formation of a 1 : 1 complex (for details see the ESI†).

The values of binding constants retrieved for the several complexes are compiled in Table S2.† Similar binding affinities with K_a values of *ca.* 10^5 M^{-1} were obtained for the several complexes studied.

Cell studies

Cytotoxic activity. The MTT assay was used to test the cytotoxic effect of the complexes by measuring the metabolic

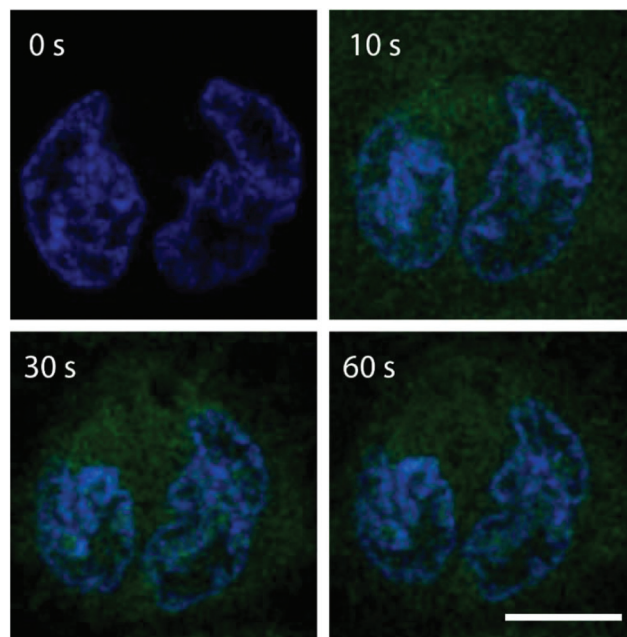


Fig. 8 Live-cell uptake of $[\text{Sm}(\text{DBM})_3(\text{NH}_2\text{Phen})]$ (2) by A2780 cells visualized by time-lapse confocal microscopy imaging. Cells were incubated with Hoechst (blue) for nuclear staining and imaged every 10 s for 1 min after the addition of $50 \mu\text{M}$ 2 (green) to the cell medium. Images acquired at time points 0, 10, 20, 30 and 60 s show single cell fluorescence distributions of the green fluorescent samarium complex for the same time points. The scale bar corresponds to $10 \mu\text{m}$.

activity of live cells, which serves as a useful and convenient marker of cellular viability. To assess the anticancer potency of the complexes, the IC_{50} values (the concentration that inhibits cell viability to 50% of the control) were determined in ovarian (A2780) and breast (MDAMB231) cancer cells after 24 h challenge with the tested compounds. The lanthanide salts 1,10-phenanthroline and 5-amine-1,10-phenanthroline, as well as cisplatin as the reference compound, were also assayed under the same conditions. The results are presented in Table 1 and Fig. S15.† The activity of the complexes was strongly dependent on the type of cancer cell, with appreciable activity against ovarian cells but modest activity in breast cells. The complexes showed a similar cytotoxic effect ($IC_{50} = 16\text{--}27\ \mu\text{M}$), being significantly more active than the corresponding ligands or lanthanide salts which displayed no effect. This trend indicates that the coordination to the metal center resulted in a considerable change and improvement of the cytotoxic activity. The lanthanide complexes showed cytotoxic effects similar to

cisplatin in both cancer cell lines, in particular for the cisplatin-sensitive A2780 cell line (Table 1). The samarium complexes displayed a similar cytotoxicity in both cell lines, while $[\text{Eu}(\text{DBM})_3(\text{NH}_2\text{Phen})]$ was the most cytotoxic complex of the series.

Cellular uptake by ICP-MS. Subcellular distribution in the A2780 cells was evaluated by ICP-MS. The lanthanide content in each cellular fraction was determined after 24 h treatment with the complexes at a concentration equivalent to their IC_{50} values in this cell line. The results presented in Fig. 7 show that the total uptake in terms of lanthanide content (ng per million cells) is quite comparable between $[\text{Sm}(\text{DBM})_3(\text{Phen})]$ and its congener $[\text{Sm}(\text{DBM})_3(\text{NH}_2\text{Phen})]$ (276 vs. 244 ng per 10^6 cells), being lower for $[\text{Tb}(\text{DBM})_3(\text{NH}_2\text{Phen})]$ (177 ng per 10^6 cells) and higher for $[\text{Eu}(\text{DBM})_3(\text{NH}_2\text{Phen})]$ (349 ng per 10^6 cells). With the exception of $[\text{Sm}(\text{DBM})_3(\text{Phen})]$, complexes were mostly retained in membrane/particulates and cytoskeleton fractions, practically to an equal extent (Fig. 7 and

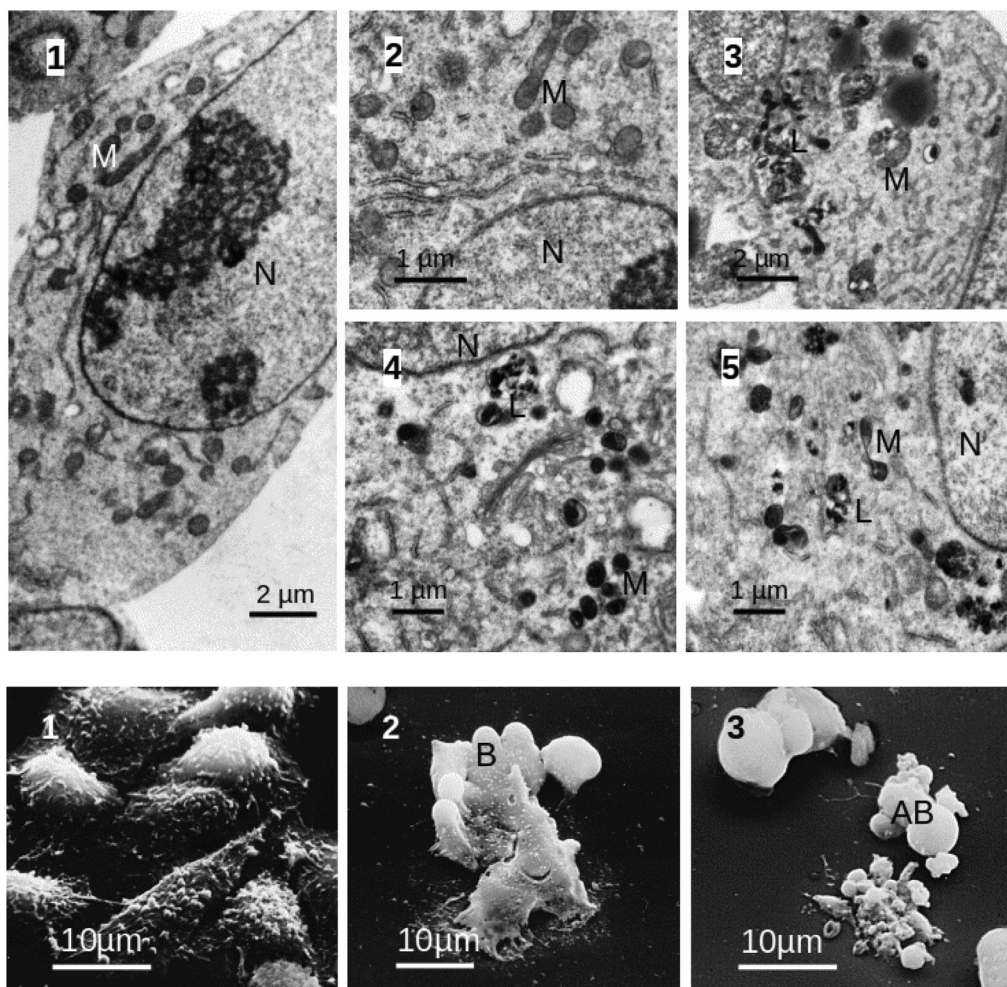


Fig. 9 A2780 cells after 24 h treatment with the lanthanide complexes at concentrations corresponding to their IC_{50} . On the top (TEM): 1 – Control (no treatment); 2 – $[\text{Sm}(\text{DBM})_3(\text{Phen})]$ (18 μM); 3 – $[\text{Eu}(\text{DBM})_3(\text{NH}_2\text{Phen})]$ (16 μM); 4 – $[\text{Tb}(\text{DBM})_3(\text{NH}_2\text{Phen})]$ (27 μM); 5 – $[\text{Sm}(\text{DBM})_3(\text{NH}_2\text{Phen})]$ (22 μM). M = mitochondria; N = nucleus; L = lysosomes. At the bottom (SEM): 1 – Control; 2 – $[\text{Sm}(\text{DBM})_3(\text{Phen})]$; 3 – $[\text{Sm}(\text{DBM})_3(\text{NH}_2\text{Phen})]$. B = cell surface blobs; AB = apoptotic bodies.

Fig. S16†). For all complexes the uptake in the nucleus is low but not negligible (4.5–8%).

The results point out that cell membranes and cytoskeleton structures could play a key role in the effects induced by these complexes, deserving further investigation due to the importance of the cytoskeleton in biological processes such as cell division, cell proliferation and cell migration.⁷²

Cellular uptake by confocal microscopy. Due to the narrow and wavelength-restricted lasers in confocal microscopy fluorescence, emission intensity is seriously restricted. Excitation at 405 nm poorly overlaps with the complexes' absorption bands and attempts to evaluate the cellular uptake by fluorescence imaging were made only for [Sm(DBM)₃(NH₂Phen)] (2) in the A2780 cells. As shown in Fig. 8, immediately after the addition of the complex (50 μM) to the medium, a diffused green staining inside the cells was observed. The complex seemed to be rapidly taken up by the cells, showing no relevant nuclear accumulation within the 30 s incubation time. Increasing the incubation times does not increase the cellular uptake and even seemed to reduce the fluorescence intensity inside the cells, most probably due to photobleaching of the samples.

Morphological alterations by TEM/SEM

Electron microscopy has been a valuable tool for investigating cells and their alterations at the ultrastructural level, which very often cannot be explored with other imaging approaches. Transmission electron microscopy (TEM) is mostly used to study the morphological alterations of cellular and subcellular compartments, while scanning electron microscopy (SEM) can be useful to reveal cell surface features.

In this work, TEM was used to investigate the effects of the lanthanide complexes on the A2780 cells. After treatment with the complexes for 24 h at a concentration equivalent to their IC₅₀, the cells presented mitochondrial alterations that were not present in the controls, usually enlargement and distortions of a few mitochondrial clusters (cells with no treatment), as can be observed in the images presented in Fig. 9. These alterations were more accentuated for the complexes with the NH₂Phen ligand. For the cells treated with these complexes, in particular with [Sm(DBM)₃(NH₂Phen)] (2), the lysosomes presented dense inclusions and the mitochondria were smaller and with a dense matrix.

The role of mitochondria and lysosomes in the mechanisms of cell death induced by the reported lanthanide complexes need further elucidation, in particular for the europium complex. By SEM and for the Sm complexes, apoptotic cells were found in the treated samples, more advanced stages of apoptotic bleb formation and cellular fragmentation being observed for 2.

Conclusions

Four Ln(III) mixed-ligand complexes containing three β-diketonate units and a phenanthroline derivative as ligands

were synthesized and characterized by analytical and spectroscopic techniques. Absorption spectroscopy showed the presence of a band at *ca.* 350 nm due to the DBM ligand for all the complexes. The luminescence emission spectra measured in DMSO show ligand centered emission bands in the visible region at *ca.* 520 nm, except for [Sm(DBM)₃(Phen)]. In PBS only sharp emission peaks were present, indicating efficient energy transfer from the excited state of the organic ligand to the emitting states of the Ln(III) ion, except for Tb(III). The UV-Vis titrations yielded apparent binding constants for the interaction of the complexes with DNA in the 10⁵ M⁻¹ range. The complexes bind DNA probably by electrostatic interactions or H-bonds between the amino group of the Phen ligands and the phosphate and sugar groups of DNA.

The complexes present a similar cytotoxic activity and a similar uptake profile with the exception of [Sm(DBM)₃(Phen)]. Interestingly, the different uptake profiles found for Sm complexes do not result in different cytotoxic activities. The NH₂Phen complexes accumulate primarily in the membrane and the cytoskeleton. A different profile was found for [Sm(DBM)₃(Phen)] that showed relatively important accumulation in the cytosol. The morphological analysis revealed that all complexes presented more pronounced mitochondrial alterations for the NH₂Phen complexes when compared with [Sm(DBM)₃(Phen)]. The Eu complex showed additional effects in the lysosomes. Interestingly, this complex was more cytotoxic than the others, particularly for longer exposure times. To sum up, the NH₂Phen ligand seems to tailor the cytotoxic effect of these complexes.

The TEM/SEM imaging techniques used in this study gave valuable insights into the biological action of the Ln(DBM)₃(RPhen) complexes. To our knowledge, these techniques have not been explored to evaluate anticancer effects exerted by this type of lanthanide-based compounds. The TEM results showed an important effect of these complexes in the mitochondria and lysosomes, in particular for the Eu complex. The elucidation of the nature of these effects remains a challenge deserving future studies, so the potential of this class of complexes as anticancer agents should be properly evaluated.

Experimental section

General materials and methods

All reagents and solvents were purchased commercially and used as received, without further purification, unless otherwise stated. Anhydrous LnCl₃ (Ln = Sm, Eu, Tb) were obtained from Alfa Aesar. 1,10-Phenanthroline monohydrate (Phen), 1,10-phenanthroline-5-amine (NH₂Phen), 1,3-diPhenyl-1,3-propanedione (HDBM), sodium hydroxide, and triethylamine were obtained from Sigma-Aldrich.

Infrared spectra were recorded on a Bruker Tensor 27 spectrometer as KBr pellets in the range 4000–400 cm⁻¹. Mass spectra were recorded in an ESI/QITMS Bruker HCT, using electrospray ionization in the positive ion mode. Elemental analyses (CHN) were performed in an automated analyzer (EA

110; CE Instruments). The ^1H and ^{13}C NMR spectra were recorded on a Varian Unity instrument operating at 300 and 75 MHz, respectively. Deuterated chloroform (CDCl_3 , ^1H $\delta_{\text{H}} = 7.26$) or acetone- d_6 (^1H , $\delta_{\text{H}} = 2.04$) were used as solvents. Chemical shifts of ^1H (δ , ppm) are reported relative to the residual solvent peaks. UV-Visible absorption spectra were recorded on a PerkinElmer Lambda 35 UV-Vis spectrophotometer with 10.0 mm quartz cuvettes. Luminescence measurements were carried out using a SPEX® Fluorolog spectrofluorimeter (Horiba Jobin Yvon) in an FL3-11 configuration, equipped with a xenon lamp and a 10.0 mm quartz cuvette. The instrumental response was corrected by means of a correction function provided by the manufacturer. The experiments were carried out at room temperature and all are all steady-state measurements.

Synthesis and characterization of lanthanide complexes

[Sm(DBM) $_3$ (Phen)] (1). Tris(dibenzoylmethane) mono(1,10-phenanthroline) samarium(III) was synthesized according to a previously reported procedure.^{56a} Its purity was checked by infrared spectroscopy, CHN elemental analyses and by ^1H NMR and ESI-MS (see the ESI†). ^1H NMR in CDCl_3 (δ , ppm) 8.27 (d, 2H, Phen), 8.20 (d, 2H, Phen), 8.03 (d, $J = 7.0$ Hz, 12H, *o*-Ph), 7.90 (d, $J = 7.2$ Hz, 2H, Phen), 7.60–7.50 (m, 18H, *m*-Ph and *p*-Ph), 7.41 (d, $J = 7.2$ Hz, 2H, Phen), 6.89 (s, 3H, CH).

[Sm(DBM) $_3$ (NH $_2$ Phen)] (2). The tris(dibenzoylmethane) mono(5-amino-1,10-phenanthroline) samarium(III) complex was synthesized according to the procedure described by Ahmed *et al.* with some adjustments.^{57b} Briefly, an ethanolic solution of 1,3-diphenylpropane-1,3-dione (183 mg, 0.81 mmol) was added to 0.82 mL of an ethanolic solution of 1 N NaOH and stirred for 30 min. Thereafter, an ethanolic solution of 5-amino-1,10-phenanthroline (52 mg; 0.27 mmol) and SmCl_3 (70 mg, 0.27 mmol) was added. The reaction mixture was stirred at 60 °C for 3 h, followed by overnight stirring at room temperature. The yellow pale precipitate formed was filtered and recrystallized from dichloromethane/*n*-hexane (188 mg; 68%). ESI-MS: m/z calcd for $[\text{M} + \text{K}]^+$ 1055.2; found 1055.5. Anal. Calc. for $\text{C}_{57}\text{H}_{42}\text{N}_3\text{O}_6\text{Sm}$ C, 67.42; H, 4.17; N, 4.14%, found C, 67.43; H 4.59; N, 4.14%. IR (KBr, ν cm^{-1}): 3462 (w), 3360 (w), 3058 (w), 1734 (w), 1634 (w), 1594 (s), 1548 (s), 1516 (s), 1492 (s), 1478 (s), 1456 (s), 1409 (s), 1310 (m), 1284 (sh, m), 1220 (w), 1179 (w), 1157 (w), 1069 (8w), 1023 (m), 748 (sh, m), 743 (w), 722 (m), 520 (w). ^1H NMR in CDCl_3 (δ , ppm) 9.62 (s, 2H, NH $_2$ Phen), 8.11 (d, $J = 7.0$ Hz, 12H, *o*-Ph), 7.98 d, $J = 7.2$ Hz (1H, NH $_2$ Phen), 7.85 (s, 3H, CH), 7.41–7.32 (m, 18H, *m*-Ph and *p*-Ph), 7.01 (s, 1H, NH $_2$ Phen), 6.91 (d, $J = 7.4$ Hz, 1H, NH $_2$ Phen), 6.78 (s, 1H, NH $_2$ Phen), 6.62 (s, 1H, NH $_2$ Phen), 4.77 (s, 1H, NH $_2$ Phen).

[Eu(DBM) $_3$ (NH $_2$ Phen)] (3). Tris(dibenzoylmethane) mono(5-amino-1,10-phenanthroline) europium(III) was synthesized and isolated in a similar way to samarium complex 2, using EuCl_3 instead of SmCl_3 . The yellow precipitate formed was filtered and recrystallized from dichloromethane/*n*-hexane (112 mg; 0.11 mmol, 50%). ESI-MS: m/z calcd for $[\text{M} + \text{Na}]^+$ 1040.2; found 1040.4. Anal. Calc. for $\text{C}_{57}\text{H}_{42}\text{N}_3\text{O}_6\text{Eu}$: C, 67.32; H, 4.16,

N, 4.13%, found C, 67.40; H 4.70; N, 4.15%. IR (KBr, ν cm^{-1}): 3443 (w), 3357 (w), 3058 (w), 1634 (sh, w), 1594 (s), 1540 (s), 1518 (s), 1493 (s), 1478 (s), 1458 (s), 149 (s), 1308 (m), 1283 (sh, m), 1219 (w), 1177 (w), 1156 (w), 1068 (m), 1023 (m), 940 (m), 926 (sh, w), 896 (w), 846 (m), 782 (m), 749 (sh, w), 721 (m), 689 (m), 682 (m), 608 (m), 513 (m). ^1H NMR in CDCl_3 (δ , ppm) 10.60 (s, 1H, NH $_2$ Phen), 10.40 (psd, 1H, NH $_2$ Phen), 10.10 (s, 1H, NH $_2$ Phen), 9.38 (s, 1H, NH $_2$ Phen), 8.78 (bs, 1H, NH $_2$ Phen), 8.63 (bs, 2H + 1H, NH $_2$ Phen) 8.40 (psd, 1H, NH $_2$ Phen), 6.90 (pss, 18H, *m*-Ph and *p*-Ph), 6.33 (pss, 12 H, *o*-Ph), 3.11 (s, 3H, CH).

[Tb(DBM) $_3$ (NH $_2$ Phen)] (4). The tris(dibenzoylmethane) mono(5-amino-1,10-phenanthroline) terbium(III) complex was synthesized by a procedure similar to that reported by Stanley *et al.*^{56b} To an ethanolic solution (15 mL) of HDBM (0.72 mmol) was added 0.73 mmol (55 μL) of 25% NH_3 and the resulting mixture was stirred in a closed boiling flask, until the smell of ammonia disappeared. Then, an aqueous solution (50 mL) of TbCl_3 (0.24 mmol) was added dropwise over a period of 30 min, with continuous stirring. The reaction was heated to 55 °C for 6 h and at room temperature for 1 h; thereafter, the solution was cooled to 0 °C and the yellow solid formed was isolated by vacuum filtration, washed with ethanol and water and vacuum dried for several hours. The recovered solid was dissolved in 5 mL of acetone and an ethanolic solution of NH $_2$ Phen (0.24 mmol) was added and stirred at 55 °C for 3 h. After cooling to room temperature, 10–15 mL of *n*-hexane were added to the solution, which was then refrigerated overnight. After filtration, 4 was obtained as a pale yellow solid (97 mg, 0.095 mmol, 40%). ESI-MS: m/z calcd for $[\text{M} + \text{Na}]^+$ 1046.2; found 1046.2 and for $[\text{M} + \text{K}]^+$ 1062.2; found 1062.5. Anal. Calc. for $\text{C}_{57}\text{H}_{42}\text{N}_3\text{O}_6\text{H}_2\text{OTb}$: C, 65.71; H, 4.26, N, 4.03%, found C, 65.78; H 4.53; N, 4.07%. IR (KBr, ν cm^{-1}): 3378 (w), 3058 (w), (w), 1634 (m), 1595 (s), 1551 (s), 1518 (s), 1493 (s), 1478 (s), 1458 (s), 1411 (s), 1384 (m), 1309 (m), 1285 (sh, m), 1220 (w), 1178 (w), 1068 (m), 1023 (m), 941 (w), 783 (sh, w), 747 (w), 721 (m), 689 (m), 609 (m), 522 (w). ^1H NMR in acetone- d_6 (δ , ppm): –46.20 (s, 1H, NH $_2$ Phen), –40.46 (s, 1H, NH $_2$ Phen), –24.15 (s, 1H, NH $_2$ Phen), –20.96 (s, 1H, NH $_2$ Phen), –18.07 (s, 1H, NH $_2$ Phen), –12.40 (s, 1H, NH $_2$ Phen) –2.21 (s, 1H, NH $_2$ Phen), 8.48 (pss, 12H, *m*-Ph), 9.30 (pss, 6H, and *p*-Ph), 13.36 (pss, 12 H, *o*-Ph), 127.30 (s, 3H, CH).

Spectroscopic measurements

The DMSO used was of spectroscopic grade from Carlo Erba. Thiazole orange, PBS (0.01 M in phosphate, NaCl 0.138 M; KCl 0.0027 M, pH 7.4 at 25° C) and ctDNA (D3664) were from Sigma.

The UV-Vis absorption luminescence spectra were measured in DMSO and PBS with solutions of *ca.* 1×10^{-5} M. The compound stock solutions were prepared in DMSO and then suitable dilutions were made, either in DMSO or PBS. The DMSO concentration is 1% or less. The stock solutions of DNA were prepared by dissolving the nucleic acid in PBS, were kept at 4 °C for about 48 h and used within two days. Solutions of DNA gave ratios of absorbance A_{260}/A_{280} of

ca. 1.9, indicating that the DNA was sufficiently protein free.^{73,74} The concentrations of the prepared *ct*DNA stock solutions were calculated based on their absorbance at 260 nm using the per nucleotide extinction coefficient $\epsilon_{260} = 6600 \text{ M}^{-1} \text{ cm}^{-1}$.⁷³ The thiazole orange (TO) solution was prepared by dissolving 1.21 mg of the compound in 5 mL of deionized water, providing a solution at 508 μM concentration, which was used on the same day. Before the addition of the complexes, DNA was saturated with thiazole orange. Selected volumes of the *ct*DNA and TO stock solutions were mixed in order to obtain a molar ratio TO/DNA of 0.8. The fluorescence emission spectra were recorded between 520 nm and 700 nm. The following parameters were used: $\lambda_{\text{exc}} = 509 \text{ nm}$, and excitation and emission bandwidths of 5 nm. Successive aliquots of the complexes' stock solutions ($1.0 \times 10^{-3} \text{ M}$) were added directly to the cuvette and the fluorescence emission spectra were recorded for each of them. Blank assays were performed for each complex where the fluorescence under the same concentrations, for TO and the complex, was recorded and subtracted from each corresponding emission spectrum. TO was added to the blank solutions since the spectra collected in the competition assay showed the development of an emission band centered at ca. 570 nm on increasing the concentrations of the complexes. In blank spectra measured for solutions containing only the complexes this band did not appear.

The UV-Vis absorption titrations with *ct*DNA were carried out by adding increasing volumes of a *ct*DNA solution (ca. 180 μM) directly to the complex solution ($1.0 \times 10^{-5} \text{ M}$, 2.5 mL) in the cuvette. The same amount was added each time to the reference cuvette.

Cell culture

Human ovarian cancer cells A2780 and human breast cancer cells MDAMB231 from the ATCC were maintained in RPMI 1640 (A2780) or Dulbecco's modified Eagle's medium (DMEM + GlutaMAXTM) supplemented with 10% fetal bovine serum and 1% penicillin/streptomycin antibiotic solution (all from Gibco Invitrogen). Cells were cultured under a humidified atmosphere of 95% air and 5% CO_2 at 37 °C (Heraeus, Germany). For the assays the cellular viability was first checked by the trypan blue dye exclusion test, and then cells were suspended in the medium and seeded further apart.

Cytotoxicity assays

The lanthanide compounds were screened for their cytotoxic activity against the ovarian and breast cancer cells within the concentration range of 10^{-7} – 10^{-4} M using the colorimetric MTT [3-(4,5-dimethylthiazol-2-yl)-2,5-diphenyltetrazolium bromide] assay, which is based on the reduction of the yellow tetrazolium salt to purple formazan by metabolically active cells. Cells were treated with the different compounds by a procedure similar to a previously described one with cells seeded in 200 μL of complete medium in 96-well plate format.⁵⁵ The compounds were first dissolved in DMSO to prepare 10 mM stock solutions. Then serial dilutions were done in complete medium. For the higher concentration of 10^{-4} M the per-

centage of DMSO was 1%, which displayed no cytotoxic effect. The commercial metallo-drug cisplatin was included in this study just for comparison. Analysis of the percentage of cell survival was carried out after 24 and 48 h cell exposures to the compounds and after incubation with MTT (0.5 mg mL^{-1} PBS). The absorbance of formazan in each well was measured at 570 nm with a plate spectrophotometer (Power Wave Xs, Bio-Tek). Each experiment was repeated at least three times and each concentration was tested in at least six replicates. Results were expressed as IC_{50} values, which were calculated using the GraphPad Prism software (v. 5.0).

Cellular uptake and distribution by ICP-MS

To measure the lanthanide content, ca. 10^6 cells per 5 mL medium were treated with the complexes at 20 μM equimolar final concentration for 24 h at 37 °C. Then the cells were washed with PBS buffer, trypsinized and centrifuged to obtain a cell pellet. Extraction of subcellular protein fractions (cytosol, nucleus, membrane/particulate, and cytoskeletal fractions) was done using a cell fractionation system (fractionPREPTM, Biovision). Each cell fraction was dissolved in 0.5 mL nitric acid (65%) in a hot plate at 100 °C for 12 h. The solution digest was diluted in ultrapure water to 10 mL, obtained from a MilliQ instrument. The lanthanide content was measured using a Thermo X-Series Quadrupole ICP-MS (Thermo Scientific), equipped with Ni cones and a glass concentric nebulizer (Meinhard, 1.0 mL min^{-1}) refrigerated with a Peltier system. Indium (¹¹⁵In) at a concentration of 10 $\mu\text{g L}^{-1}$ was used as an internal standard. Standards were prepared from multi-elemental ICP-MS 71 A or, for Tb, ICP-MS MSTB-10PPM-125MS (Inorganic Venture) with a final concentration of 5.0% nitric acid. The following quality control was applied: the internal standard showed variations between 80 and 120%; the blank's concentrations were inferior to the limit of detection (1 $\mu\text{g L}^{-1}$) and the sample duplicates don't differ more than 10%.

Cellular uptake by confocal fluorescence microscopy

Cellular uptake of $[\text{Sm}(\text{DBM})_3(\text{NH}_2\text{Phen})]$ was visualized by time-lapse confocal microscopy imaging of live A2780 cells. Briefly, cells in the medium were seeded on sterile 35 mm Petri dishes (MatTek, Ashland, MA, USA) at a density of approximately 10^5 cells per mL. After 24 h incubation at 37 °C the cells were labelled with Hoechst 33342 (Molecular Probes, Eugene, OR, USA) at 1 μL per 2 mL of medium for 5 min at 37 °C. Hoechst 33342 is a cell permeant nuclear probe that emits blue fluorescence when bound to DNA. After labelling, the cells were washed three times with medium and maintained in DMEM/F12 without Phenol red for live imaging experiments. Cells were imaged using a Zeiss LSM 710 inverted laser scanning confocal microscope (Carl Zeiss, Germany) equipped with a large incubator for 37 °C temperature control (Pecan, Germany) using a PlanApochromat 63 \times /1.4 oil-immersion objective. Hoechst fluorescence was detected using a 405 nm diode laser (30 mW nominal output) for excitation and a 425–485 nm spectral detection window. The fluorescence of

the lanthanide compound was detected using the same 405 nm violet laser and a 543–797 nm detection window. The pinhole aperture was adjusted in both channels to achieve the same optical slice thickness (1 μm). After the addition of the lanthanide complex to the cell medium, 50 μM (final conc.), sequential images in both green (lanthanide compound) and blue (Hoechst) channels were then acquired every 10 s for 60 s time period.

Morphological analysis by TEM

A2780 cells at approximately 70% confluence were treated with 20 μM Ln complexes at 37 $^{\circ}\text{C}$ for 24 h. Untreated cells were used as the controls. After incubation, the culture medium was discarded and replaced by 5 mL of the primary fixative that consisted of 3% glutaraldehyde in 0.1 M sodium cacodylate buffer pH 7.3. Following primary fixation for 2 h at 4 $^{\circ}\text{C}$, cells were scrapped, pelleted and embedded in 2% agar for further processing. The samples were washed in cacodylate buffer and secondarily fixed for 3 h in 1% osmium tetroxide in 0.1 M sodium cacodylate buffer pH 7.3. Then samples were washed with 0.1 M acetate buffer, pH 5.0, and further fixed with 0.5% uranyl acetate in the same buffer for 1 h. Dehydration was carried out in increasing concentrations of ethanol. After passing through propylene oxide, the samples were embedded in Epon-Araldite using SPI-Pon as an Epon 812 substitute. Thin sections were prepared with glass or diamond knives and stained with 2% aqueous uranyl acetate and Reynold's lead citrate. The stained sections were studied and photographed using a JEOL 100-SX electron microscope.

Morphological analysis by SEM

Cell samples grown in coverslips and treated as stated in the above section ("Morphological analysis by TEM") were fixed for 2 h in 3% glutaraldehyde in 0.1 M sodium cacodylate buffer at pH 7.3. The cells were then dehydrated in increasing concentrations of ethanol, passed through liquid *t*-butanol at 40 $^{\circ}\text{C}$ for 2 \times 10 minutes and then the *t*-butanol was solidified in a refrigerator at 4 $^{\circ}\text{C}$. Solid *t*-butanol was removed by sublimation under vacuum in a vacuum excavator for 2 h. The dried cell layers were covered with gold in a JEOL JEE-4X vacuum evaporator and observed using a JEOL JSM-5400 scanning electron microscope.

Conflicts of interest

There are no conflicts of interest to declare.

Acknowledgements

The authors acknowledge financial support from the Portuguese Fundação para a Ciência e Tecnologia (FCT) (grant no. UID/QUI/00100/2013, UID/MULTI/04349/2013 and UID/BIO/04565/2013). Isabel Correia thanks FCT for the program Investigador FCT.

References

- 1 M. O. F. Khan, M. J. Deimling and A. Philip, Medicinal Chemistry and the Pharmacy Curriculum, *Am. J. Pharm. Educ.*, 2011, **75**, 161.
- 2 A.-M. Florea and D. Büsselberg, Cisplatin as an anti-tumor drug: Cellular mechanisms of activity, drug resistance and induced side effects, *Cancers*, 2011, **3**, 1351–1371.
- 3 M. Frezza, S. Hindo, D. Chen, A. Davenport, S. Schmitt, D. Tomco and Q. P. Dou, Novel metals and metal complexes as platforms for cancer therapy, *Curr. Pharm. Des.*, 2010, **16**, 1813–1825.
- 4 S. Dasari and P. B. Tchounwou, Cisplatin in cancer therapy: Molecular mechanisms of action, *Eur. J. Pharmacol.*, 2014, **740**, 364–378.
- 5 J. C. Pessoa, S. Etcheverry and D. Gambino, Vanadium compounds in medicine, *Coord. Chem. Rev.*, 2015, **301–302**, 24–48.
- 6 S. Medici, M. Peana, V. M. Nurchi, J. I. Lachowicz, G. Crisponi and M. A. Zoroddu, Noble metals in medicine: Latest advances, *Coord. Chem. Rev.*, 2015, **284**, 329–350.
- 7 P. Chellan and P. J. Sadler, The elements of life and medicines, *Philos. Trans. R. Soc., A*, 2015, **373**, 20140182.
- 8 J. Lopes, D. Alves, T. S. Morais, P. J. Costa, M. F. Piedade, F. Marques, M. J. Villa de Brito and M. H. Garcia, New copper(i) and heteronuclear copper(i)-ruthenium(ii) complexes: Synthesis, structural characterization and cytotoxicity, *J. Inorg. Biochem.*, 2017, **169**, 68–78.
- 9 I. E. Leon, J. F. Cadavid-Vargas, A. L. Di Virgilio and S. B. Etcheverry, Vanadium, ruthenium and copper compounds: A new class of nonplatinum metallodrugs with anticancer activity, *Curr. Med. Chem.*, 2017, **24**, 112–148.
- 10 C. Nardon, G. Boscutti and D. Fregona, Beyond platinum: Gold complexes as anticancer agents, *Anticancer Res.*, 2014, **34**, 487–492.
- 11 U. Ndagi, N. Mhlongo and M. E. Soliman, Metal complexes in cancer therapy - an update from drug design perspective, *Drug Des., Dev. Ther.*, 2017, **11**, 599–616.
- 12 C. G. Hartinger, M. A. Jakupec, S. Zorbas-Seifried, M. Groessl, A. Egger, W. Berger, H. Zorbas, P. J. Dyson and B. K. Keppler, KP1019, A new redox-active anticancer agent -preclinical development and results of a clinical phase I study in tumor patients, *Chem. Biodivers.*, 2008, **5**, 2140–2155.
- 13 A. Levina, A. Mitra and P. A. Lay, Recent developments in ruthenium anticancer drugs, *Metallomics*, 2009, **1**, 458–470.
- 14 S. Leijen, S. A. Burgers, P. Baas, D. Pluim, M. Tibben, E. van Werkhoven, E. Alessio, G. Sava, J. H. Beijnen and J. H. M. Schellens, Phase I/II study with ruthenium compound NAMI-A and gemcitabine in patients with non-small cell lung cancer after first line therapy, *Invest. New Drugs*, 2015, **33**, 201–214.
- 15 V. Brabec and O. Nováková, DNA binding mode of ruthenium complexes and relationship to tumor cell toxicity, *Drug Resist. Updates*, 2006, **9**, 111–122.

- 16 N. Graf and S. J. Lippard, Redox activation of metal-based prodrugs as a strategy for drug delivery, *Adv. Drug Delivery Rev.*, 2012, **64**, 993–1004.
- 17 L. Côte-Real, F. Mendes, J. Coimbra, T. S. Morais, A. I. Tomaz, A. Valente, M. H. Garcia, I. Santos, M. Bicho and F. Marques, Anticancer activity of structurally related ruthenium(II) cyclopentadienyl complexes, *J. Biol. Inorg. Chem.*, 2014, **19**, 853–867.
- 18 L. Côte-Real, A. P. Matos, I. Alho, T. S. Morais, A. I. Tomaz, M. H. Garcia, I. Santos, M. P. Bicho and F. Marques, Cellular uptake mechanisms of an antitumor ruthenium compound: the endosomal/lysosomal system as a target for anticancer metal-based drugs, *Microsc. Microanal.*, 2013, **19**, 1122–1130.
- 19 A. C. Komor and J. K. Barton, The path for metal complexes to a DNA target, *Chem. Commun.*, 2013, **49**, 3617–3630.
- 20 S. Spreckelmeyer, C. Orvig and A. Casini, Cellular transport mechanisms of cytotoxic metallodrugs: An overview beyond cisplatin, *Molecules*, 2014, **19**, 15584–15610.
- 21 R. D. Teo, J. Termini and H. B. Gray, Lanthanides: Applications in cancer diagnosis and therapy, *J. Med. Chem.*, 2016, **59**, 6012–6024.
- 22 A. Cârâc, Biological and biomedical applications of the lanthanides compounds: A mini review, *Proc. Rom. Acad., Ser. B: Chem., Life Sci. Geosci.*, 2017, **19**, 69–74.
- 23 M. P. C. Campello, S. Lacerda, I. C. Santos, G. A. Pereira, C. F. G. C. Geraldes, J. Kotek, P. Hermann, J. Vaněk, P. Lubal, V. Kubiček, E. Tot and I. Santos, Lanthanide(III) complexes of 4,10-Bis(phosphonomethyl)-1,4,7,10-tetraazacyclododecane-1,7-diacetic acid (trans-H6do2a2p) in solution and in the solid state: Structural studies along the series, *Chem. – Eur. J.*, 2010, **16**, 8446–8465.
- 24 J.-C. G. Bünzli, Rising stars in science and technology: Luminescent lanthanide materials, *Eur. J. Inorg. Chem.*, 2017, 5058–5063.
- 25 S. I. Weissman, Intramolecular energy transfer the fluorescence of complexes of europium, *J. Chem. Phys.*, 1942, **10**, 214–217.
- 26 A. J. Amoroso and S. J. A. Pope, Using lanthanide ions in molecular bioimaging, *Chem. Soc. Rev.*, 2015, **44**, 4723–4742.
- 27 F. Marques, K. P. Guerra, L. Gano, J. Costa, M. P. Campello, L. M. P. Lima, R. Delgado and I. Santos, 153Sm and 166Ho complexes with tetraaza macrocycles containing pyridine and methylcarboxylate or methylphosphonate pendant arms, *J. Biol. Inorg. Chem.*, 2004, **9**, 859–872.
- 28 S. N. Misra, M. A. Gagnani, I. D. M and R. S. Shukla, Biological and clinical aspects of lanthanide coordination compounds, *Bioinorg. Chem. Appl.*, 2004, **2**, 155–192.
- 29 R. D. Teo, J. Termini and H. B. Gray, Lanthanides: Applications in cancer diagnosis and therapy, *J. Med. Chem.*, 2016, **59**, 6012–6024.
- 30 J.-C. G. Bünzli, Lanthanide luminescence for biomedical analyses and imaging, *Chem. Rev.*, 2010, **110**, 2729–2755.
- 31 A. K. Hagan and T. Zuchner, Lanthanide-based time-resolved luminescence immunoassays, *Anal. Bioanal. Chem.*, 2011, **400**, 2847–2864.
- 32 J. Sahoo, P. S. Subramanian and S. Jaiswar, Synthesis and Characterization of Ln(III) Complexes and its Luminescence Properties, *J. Fluoresc.*, 2016, **26**, 1341–1347.
- 33 J. Lohrke, T. Frenzel, J. Endrikat, F. C. Alves, T. M. Grist, M. Law, J. M. Lee, T. Leiner, K.-C. Li, K. Nikolaou, M. R. Prince, H. H. Schild, J. C. Weinreb, K. Yoshikawa and H. Pietsch, 25 years of contrast-enhanced MRI: developments, current challenges and future perspectives, *Adv. Ther.*, 2016, **33**, 1–28.
- 34 P. Anderson, Samarium for osteoblastic bone metastases and osteosarcoma, *Expert Opin. Pharmacother.*, 2006, **7**, 1475–1486.
- 35 M. S. Hofman, M. Michael, R. J. Hicks and P. MacCallum, 177Lu-Dotatate for midgut neuroendocrine tumors, *N. Engl. J. Med.*, 2017, **376**, 1390–1392.
- 36 C. Shiju, D. Arish and S. Kumaresan, Synthesis, characterization, cytotoxicity, DNA cleavage, and antimicrobial activity of lanthanide(III) complexes of a Schiff base ligand derived from glycyglycine and 4-nitrobenzaldehyde, *Arabian J. Chem.*, 2017, **10**, S2584–S2591.
- 37 Z.-Q. Xu, X.-J. Mao, L. Jia, J. Xu, T.-F. Zhu, H.-X. Cai, H.-Y. Bie, R.-H. Chen and T.-L. Ma, Synthesis, characterization and anticancer activities of two lanthanide(III) complexes with a nicotinohydrazone ligand, *J. Mol. Struct.*, 2015, **1102**, 86–90.
- 38 L.-F. Chu, Y. Shi, D.-F. Xu, H. Yu, J.-R. Lin and Q.-Z. He, Synthesis and biological studies of some lanthanide complexes of schiff base, *Synth. React. Inorg. Met.-Org. Chem.*, 2015, **45**, 1617–1626.
- 39 (a) A. Hussain, S. Gadadhar, T. K. Goswami, A. A. Karande and A. R. Chakravarty, Photoactivated DNA cleavage and anticancer activity of pyrenyl-terpyridine lanthanide complexes, *Eur. J. Med. Chem.*, 2012, **50**, 319–331; (b) A. Hussain and A. R. Chakravarty, Photocytotoxic lanthanide complexes, *J. Chem. Sci.*, 2012, **124**, 1327–1342; (c) A. Hussain, S. Gadadhar, T. K. Goswami, A. A. Karande and A. R. Chakravarty, Photo-induced DNA cleavage activity and remarkable photocytotoxicity of lanthanide(III) complexes of a polypyridyl ligand, *Dalton Trans.*, 2012, **41**, 885–895; (d) A. Hussain, K. Somyajit, B. Banik and S. Banerjee, Enhancing the photocytotoxic potential of curcumin on terpyridyl lanthanide(III) complex formation, *Dalton Trans.*, 2013, **42**, 182–195.
- 40 S. Dasari, S. Singh, S. Sivakumar and A. K. Patra, Dual-Sensitized Luminescent Europium(III) and Terbium(III) Complexes as Bioimaging and Light-Responsive Therapeutic Agents, *Chem. – Eur. J.*, 2016, **22**, 17387–17396.
- 41 (a) J. C.-G. Bünzli and C. Piguet, Taking advantage of luminescent lanthanide ions, *Chem. Soc. Rev.*, 2005, **34**, 1048–1077; (b) J.-C.G. Bünzli, Lanthanide luminescence for biomedical analyses and imaging, *Chem. Rev.*, 2010, **110**, 2729–2755.
- 42 X. Wang, H. Chang, J. Xie, B. Zhao, B. Liu, S. Xu, W. Pei, N. Ren, L. Huang and W. Huang, Recent developments in lanthanide-based luminescent probes, *Coord. Chem. Rev.*, 2014, **273–274**, 201–212.
- 43 T. Terai, K. Kikuchi, S.-Y. Iwasawa, T. Kawabe, Y. Hirata, Y. Urano and T. Nagano, Modulation of luminescence

- intensity of lanthanide complexes by photoinduced electron transfer and its application to a long-lived protease probe, *J. Am. Chem. Soc.*, 2006, **128**, 6938–6946.
- 44 S. Shuvaev, M. Starck and D. Parker, Responsive, water-soluble europium(III) luminescent probes, *Chem. – Eur. J.*, 2017, **23**, 9974–9989.
- 45 M. P. Coogan and V. Fernandez-Moreira, Progress with, and prospects for, metal complexes in cell imaging, *Chem. Commun.*, 2014, **50**, 384–399.
- 46 K. Binnemans, Rare-earth beta-diketonates, in *Handbook on the Physics and Chemistry of Rare Earths*, ed. K. A. Gschneidner Jr., J.-C. G. Bünzli and V. K. Pecharsky, Elsevier, vol. 35, 2005.
- 47 J. Zaharieva, M. Milanova and D. Todorovsky, Synthesis conditions impact on the composition, structure, and fluorescence properties of the europium dibenzoylmethane complexes, *Synth. React. Inorg., Met.-Org., Nano-Met. Chem.*, 2010, **40**, 651–661.
- 48 M. Milanova, J. Zaharieva, I. Manolov, M. Getzova and D. Todorovsky, Lanthanide complexes with β -diketones and coumarin derivatives: synthesis, thermal behaviour, optical and pharmacological properties and immobilization, *J. Rare Earths*, 2010, **28**(Spec. Issue), 66–74.
- 49 S. I. Weissman, Intramolecular energy transfer the fluorescence of complexes of europium, *J. Chem. Phys.*, 1942, **10**, 214–217.
- 50 J. Benítez, L. Becco, I. Correia, S. M. Leal, H. Guiset, J. C. Pessoa, J. Lorenzo, S. Tanco, P. Escobar, V. Moreno, B. Garat and D. Gambino, Vanadium polypyridyl compounds as potential antiparasitic and antitumoral agents: new achievements, *J. Inorg. Biochem.*, 2011, **105**, 303–312.
- 51 I. Correia, S. Roy, C. P. Matos, S. Borovic, C. Butenko, I. Cavaco, F. Marques, J. Lorenzo, A. Rodríguez and V. Moreno, and J. C. Pessoa, Vanadium(IV) and copper(II) complexes of salicylaldehydes and aromatic heterocycles: Cytotoxicity, DNA binding and DNA cleavage properties, *J. Inorg. Biochem.*, 2015, **147**, 134–146.
- 52 F. Marques, A. P. Matos, C. P. Matos, I. Correia, J. C. Pessoa and M. P. Campello, Ultrastructural features of cells following incubation with metal complexes using Phenanthroline-based ligands: The influence of the metal center, *Ultrastruct. Pathol.*, 2017, **41**, 128–129.
- 53 C. Acilan, B. Cevatemre, Z. Adiguzel, D. Karakas, E. Ulukaya, N. Ribeiro, I. Correia and J. C. Pessoa, Synthesis, biological characterization and evaluation of molecular mechanisms of novel copper complexes as anti-cancer agents, *Biochim. Biophys. Acta*, 2017, **1861**, 218–234.
- 54 G. Scalese, M. F. Mosquillo, S. Rostán, J. Castiglioni, I. Alho, L. Pérez, I. Correia, F. Marques, J. C. Pessoa and D. Gambino, Heteroleptic oxidovanadium(IV) complexes of 2-hydroxynaphthylaldimine and polypyridyl ligands against *Trypanosoma cruzi* and prostate cancer cells, *J. Inorg. Biochem.*, 2017, **175**, 154–166.
- 55 G. Scalese, I. Correia, J. Benítez, S. Rostán, F. Marques, F. Mendes, A. P. Matos, J. C. Pessoa and D. Gambino, Evaluation of cellular uptake, cytotoxicity and cellular ultra-structural effects of heteroleptic oxidovanadium(IV) complexes of salicylaldehydes and polypyridyl ligands, *J. Inorg. Biochem.*, 2017, **166**, 162–172.
- 56 (a) N. J. R. Melby, E. Abramson and J. C. Caris, Synthesis and Fluorescence of Some Trivalent Lanthanide Complexes, *J. Am. Chem. Soc.*, 1964, **86**, 5117–5125; (b) J. M. Stanley, C. K. Chan, X. Yang, R. A. Jones and B. J. Holliday, Synthesis, X-ray crystal structure and photophysical properties of tris(dibenzoylmethanido)(1,10-Phenanthroline)samarium(III), *Polyhedron*, 2010, **29**, 2511–2515.
- 57 (a) Z. Ahmed and K. Iftikhar, Synthesis, luminescence and NMR studies of lanthanide (III) complexes with hexafluoroacetylacetone and Phenanthroline. Part II, *Inorg. Chim. Acta*, 2012, **392**, 165–176; (b) Z. Ahmed and K. Iftikhar, Solution studies of lanthanide (III) complexes based on 1,1,1,5,5,5-hexafluoro-2,4-pentanedione and 1,10-Phenanthroline Part-I: Synthesis, ^1H NMR, 4f–4f absorption and photoluminescence, *Inorg. Chim. Acta*, 2010, **363**, 2606–2615.
- 58 I. Malina, N. Juhnevics and V. Kampars, Study of thermal and optical properties of dibenzoylmethane Eu(III) organic complexes, *Proc. Est. Acad. Sci.*, 2017, **66**, 493–500.
- 59 E. E. S. Teotonio, H. F. Brito, G. F. Sá, M. C. F. C. Felinto, R. H. A. Santos, R. M. Fuquen, I. F. Costa, A. R. Kennedy, D. Gilmore and W. M. Faustino, Structure and luminescent investigation of the Ln(III)– β -diketonate complexes containing tertiary amides, *Polyhedron*, 2012, **38**, 58–67.
- 60 J. Li, H. Li, P. Yan, P. Chen, G. Hou and G. Li, Synthesis, Crystal Structure, and Luminescent Properties of 2-(2,2,2-Trifluoroethyl)-1-indone Lanthanide Complexes, *Inorg. Chem.*, 2012, **51**, 5050–5057.
- 61 Z. Zeng, J. Wen, H. Yan, Z. Liu, Y. Xu, H. Li, C. Zhong, F. Liu and S. Sun, A simple photoluminescent strategy for pH and amine vapors detection based on Eu(III)-complex functionalized material, *RSC Adv.*, 2016, **6**, 37385–37390.
- 62 S. F. Tayyari, H. Rahemi, A. R. Nekoei, M. Zahedi-Tabrizi and Y. A. Wang, Vibrational assignment and structure of dibenzoylmethane: A density functional theoretical study, *Spectrochim. Acta, Part A*, 2007, **66**, 394–404.
- 63 R. C. Smith, *Infrared spectra of substituted 1,10-Phenanthrolines*. Retrospective Theses and Dissertations. Paper 2419, 1961.
- 64 S. V. Eliseeva and J.-C. G. Bünzli, *Chem. Soc. Rev.*, 2010, **39**, 189–227.
- 65 Y. Luo, Q. Yan, S. Wu, W. Wu and Q. Zhang, Inter- and intra-molecular energy transfer during sensitization of Eu(DBM)3Phen luminescence by Tb(DBM)3Phen in PMMA, *J. Photochem. Photobiol., A*, 2007, **191**, 91–96.
- 66 C. Xu, *Monatsh. Chem.*, 2010, **141**, 631–635.
- 67 G. Accorsi, A. Listorti, K. Yoosaf and N. Armaroli, 1,10-phenanthrolines: versatile building blocks for luminescent molecules, materials and metal complexes, *Chem. Soc. Rev.*, 2009, **38**, 1690–1700.
- 68 M. Khorasani-Motlagh, M. Noroozifar, A. Moodi and S. Niroomand, Fluorescence studies, DNA binding properties and antimicrobial activity of a dysprosium(III)

- complex containing 1,10-phenanthroline, *J. Photochem. Photobiol., B*, 2013, **127**, 192–201.
- 69 Z. Nie, H. Lee, H. Shin, H. Lee, K. S. Lim and M. Lee, Optical properties and spectroscopy parameters of Sm(DBM)(3)Phen-doped poly(methyl methacrylate), *Spectrochim. Acta, Part A*, 2009, **72**, 554–560.
- 70 K. Binnemans, Interpretation of europium(III) spectra, *Coord. Chem. Rev.*, 2015, **295**, 1–45.
- 71 J. Nygren, N. Svanvik and M. Kubista, The interactions between the fluorescent dye thiazole orange and DNA, *Biopolymers*, 1998, **46**, 39–51.
- 72 M. Trendowski, Exploiting the cytoskeletal filaments of neoplastic cells to potentiate a novel therapeutic approach, *Biochim. Biophys. Acta*, 2014, **1846**, 599–616.
- 73 J. M. Teare, R. Islam, R. Flanagan, S. Gallagher, M. G. Davies and C. Grabau, Measurement of nucleic acid concentrations using the DyNA Quant and the GeneQuant, *BioTechniques*, 1997, **22**, 1170–1174.
- 74 S. R. Gallagher, in *Current Protocols in Molecular Biology*, ed. F. A. Ausubel, R. Brent, R. E. Kingston, D. D. Moore, J. G. Seidman, J. A. Smith and K. Struhl, John Wiley & Sons, New York, 1989.